Preprints.org

Article

Vibrio cholerae Gut Colonization of Zebrafish Larvae Induces Differential Behavior Responses

Isabella Cubillejo , Kevin R Theis , Jonathan Panzer , Xixia Luo , Shreya Banerjee , Ryan Thummel , Jeffrey H Withey [*]

Article

*Vibrio cholera*e Gut Colonization of Zebrafish Larvae Induces Differential Behavior Responses

Isabella Cubillejo [1], Kevin R Theis [1], Jonathan Panzer [1], Xixia Luo [2], Shreya Banerjee [2], Ryan Thummel [2] and Jeffrey H Withey [1,*]

[1] Department of Biochemistry, Microbiology, and Immunology, Wayne State University, Detroit, Michigan, USA

[2] Department of Ophthalmology, Visual and Anatomical Sciences, Wayne State University School of Medicine, Detroit, Michigan, USA

* Jeffrey H. Withey: jwithey@med.wayne.edu

Abstract: Cholera is a diarrheal disease prevalent in populations without access to clean water. Cholera is caused by *Vibrio cholerae*, which colonizes the upper small intestine in humans once ingested. A growing number of studies suggests the gut microbiome composition modulates animal behavior. Zebrafish are an established cholera model that can maintain a complex, mature gut microbiome during infection. Larval zebrafish, which have immature gut microbiomes, provide the advantage of high-throughput analyses for established behavioral models. We identified the effects of *V. cholerae* O1 El Tor C6706 colonization at 5 days post-fertilization (dpf) on larval zebrafish behavior by tracking startle responses at 10 dpf. We also characterized the larval gut microbiome using 16S rRNA sequencing. *V. cholerae*-infected or uninfected control groups were exposed to either an alternating light/dark stimuli or a single-tap stimulus, and average distance and velocity were tracked. While there was no significant difference in the light/dark trial, we report a significant decrease in distance moved for C6706-colonized larvae during the single-tap trial. This suggests that early *V. cholerae* colonization of the larval gut microbiome has a dampening effect on sensorimotor function, supporting the idea of a link between the gut microbiome and behavior.

Keywords: *Vibrio cholerae*; cholera; zebrafish larvae; microbiome; behavior

1. Introduction

Cholera is a profuse diarrheal disease spread via the fecal-oral route through contaminated food and water and is endemic in communities around the world without potable water and sanitary facilities [1]. Cholera patients pass a characteristic "rice-water stool" and, without rehydration treatment, are at risk of severe dehydration and death [2]. The World Health Organization estimates an annual 1-4 million cholera cases and upwards of 100,000 deaths internationally, with the most vulnerable demographic being children younger than 5 years old [3,4]. The global risk of cholera is characterized as very high, due to the increasing number of outbreaks and lack of vaccine availability; prevalence is expected to worsen with climate change [5,6].

Vibrio cholerae, the etiological agent, is a motile Gram-negative bacillus found in aquatic environments [7,8]. *V. cholerae* isolates are classified into over 200 serogroups based on the somatic O-antigen. Some serogroups may cause mild to severe diarrheal symptoms, but only serogroups O1 and O139 are pandemic [1,8]. The O1 serogroup is further divided into two biotypes, classical and El Tor. The toxin-coregulated pilus (TCP) and cholera toxin (CT) are the two major virulence factors unique to these biotypes. These allow *V. cholerae* to colonize the upper small intestinal epithelium in humans and induce severe diarrheal symptoms, respectively [1,9–12]. Classical strains were the cause of the first six cholera pandemics beginning in 1817. However, beginning in 1961 El Tor became the dominant if not primary cause of the current seventh pandemic [13]. In comparison to El Tor strains, classical strains cause more severe diarrheal symptoms. However, El Tor strains are thought to be

more persistent in colonization, as infection duration lasts longer [9,14]. Currently, some circulating El Tor strains, known as atypical or variant El Tor, have acquired some of the classical biotype virulence traits and cause more severe symptoms [15–17].

The human gut microbiome contains the majority of commensal bacteria in the body, that are crucial to digestion, nutrient absorption, metabolism, and the immune system [18,19]. Firmicutes and Bacteroidetes are normally the dominant phyla of the human gut microbiome, though individual variation occurs due to genetics, age, sex, diet, and lifestyle, among other factors [20–22]. The mucus layer of the gut epithelium is essential to maintain a diverse microbiome, as it provides a surface for the resident gut microbiota and contains proteins for the bacteria to metabolize [23–25]. During cholera infection, *V. cholerae* colonizes the upper small intestine [11,26]. Here, CT induces physical efflux of ions and water, and the mucus shedding in tandem drastically decreases gut microbiome diversity. At this stage, *V. cholerae* are the most abundant bacteria in the now-altered human gut, and resident gut microbiota fluctuate in response to colonization [27,28].

Growing evidence suggests that dysbiosis (a significant change in the microbiome composition) of the gut is implicated in neurological conditions such as anxiety, depression, autism, and Parkinson's [29–31]. Additionally, presence of a microbiome is necessary for normal neurological development [32,33]. Because *V. cholerae* colonizes and perturbs the gut microbiome, it may be possible that infection affects neurological activity in a similar manner.

Current mammalian animal models used to study *V. cholerae* are useful for understanding pathogenesis, but require invasive procedures, use of infant animals, or antibiotic-treated adult animals to enable *V. cholerae* to colonize the gut [34–39]. Larval and adult zebrafish have been established as natural host models for *V. cholerae*, as infection is done via immersion, and zebrafish exhibit diarrheal symptoms similar to humans [40–42]. The zebrafish gut microbiome shifts over time among individuals and, without the use of antibiotics or invasive procedures required of other animal models, zebrafish have a mature gut microbiome before and during *V. cholerae* colonization [40,43–45]. Adult zebrafish will clear the *V. cholerae* infection on their own, and the duration varies based on the biotype strain used: classical strains are cleared within 72 hours post-infection (hpi), and El Tor strains can colonize beyond 144 hpi [40]. Unpublished data from our lab suggests El Tor persists for up to two weeks. Zebrafish larvae can also be infected via immersion at 5 days post-fertilization (dpf), when the gut opens and uptake of exogenous food begins [40,46]. The larval gut microbiome is primarily colonized by bacteria of the phylum Pseudomonadota [43,47].

Previous studies have found that microbial colonization is required in germ-free zebrafish larvae for normal swim behavior and neurobehavioral development [48,49]. One study found that axenic zebrafish larvae infected with *V. cholerae* at 1 dpf exhibited a decrease in hypoactivity at 10 dpf, while conventionally colonized zebrafish larvae infected with *V. cholerae* had no change in locomotor activity [49]. However, this was tested with a dark/light paradigm, whereas a second assay testing for a separate stimulus response would be beneficial to examining gut microbiome crosstalk with different regions of the larval brain and nervous system. An alternating light/dark assay tests the visual system, and a single-tap trial would test locomotor function separate from the visual system. Here, we report *V. cholerae* El Tor C6706 colonization of the larval zebrafish gut has no effect on the response to a visual stimulus, but a dampening effect on the response to an acoustic stimulus.

2. Materials and Methods

2.1. Zebrafish Husbandry

Wild-type AB larvae were used, and larvae were fasted at least 12 h before behavioral trials. During experimentation, larvae were placed in autoclaved water from the Aquaneering aquatic housing system filtered by reverse osmosis and maintained at pH 7.0 to 7.5. Tank water was conditioned with Instant Ocean salt (Aquarium Systems, Mentor, OH) to a conductivity of 600 to 700 µS. Fish were kept in a glass-front incubator at 28°C on a timed 14 hour light, 10 hour dark cycle. All animal protocols were approved by the Wayne State University IACUC.

2.2. Vibrio cholerae Infection

V. cholerae infection of zebrafish has been previously described [40,41]. Briefly, El Tor C6706 was incubated with aeration in 30 mL of Luria Broth (LB) agar with 100 µg/mL streptomycin at 37ºC for 12-14 hours. Cells were centrifuged at 8000g, washed and resuspended with 1x phosphate buffer saline (PBS) to a concentration of 10^9 CFU/mL by measuring at OD600 nm. Serial dilutions were plated onto LB agar with 100 µg/mL streptomycin and 100 µg/mL X-galactosidase (X-gal) for confirmation. In 6-well plates (Fisher Scientific, Pittsburgh, PA) the *V. cholerae* dilution was pipetted into 5 mL of autoclaved water from the Aquaneering system to an average concentration for both behavioral trials, each repeated in triplicate, of 1.16×10^7 CFU per well. For the uninfected group in separate 6-well plates, the same amount of sterile 1x PBS was used.

Approximately 10-15 larvae at 5 dpf were then placed in each well with the inoculum (uninfected n=88, C6706 n=111). After 6 hpi, all larvae from both groups were removed from wells and separately placed in new wells with 5 mL of new autoclaved water. This rinsing process was repeated three times to wash off the initial inoculum as thoroughly as possible. The larvae were then placed in beakers with 80 mL of new autoclaved water. At 24 hpi larvae were fed larval food (ARTEMAC, Aquafauna Bio-Marine). A water change, rinsing, and feeding were repeated daily following infection. Additionally, 100 µL of water from each experimental beaker was plated directly onto LB Agar with 100 µg/mL streptomycin and 100 µg/mL X-gal daily, to confirm continued *V. cholerae* infection of C6706 group, and sterility of uninfected group. At 9 dpf, individual larvae were placed in flat bottom 24-well plates (diameter 1.65 inch wells) (Falcon, MA) to acclimate for 24 hours. At 10 dpf, or 5 days post-infection (dpi), all 24-well plates were closed with a lid and sealed in parafilm around the edges, and light-dark or single-tap stimulus trials were performed.

2.3. Behavioral Assays

All behavioral assays were performed as previously described [50]. Briefly, the larvae in 24-well plates sealed with parafilm were placed in a DanioVision Observation Chamber (Noldus Information Technology, Wageningen, Netherlands) and tracked using the EthoVision XT13 software and a Basler Gen1 Camera (Basler acA1300-60). Camera resolution was set at 1280×960 and the frame rate was set at 25. The DanioVision Temperature Control Unit maintained the larvae at a constant temperature of 28.0±0.5 °C via a steady flow of water to the chamber. All behavioral trials were performed from 1-4 PM. Both behavioral assays were repeated in triplicate.

2.4. Light/Dark Trial

Larvae acclimated in the Noldus in darkness for 12 minutes. After acclimation, recording began and lasted for 24 minutes. A uniform light was emitted at 10,500 lux from below the stage. During all 4 alternating cycles of 3 minutes light and 3 minutes dark, distance moved (cm) and velocity (cm/sec) were tracked (uninfected n=25, C6706 n=60). Average distance and average velocity were calculated in Excel from 30 second time bins and analyzed on GraphPad using Mann-Whitney test with $p < 0.05$ as cutoff for significance.

2.5. Single-Tap Trial

Larvae acclimated in the Noldus in darkness for 12 minutes. After acclimation, recording began and lasted for 2 minutes. Larvae were exposed to 1 minute of no stimulation, followed by a single-tap at the highest intensity setting, and ending with 1 minute of no stimulation. Distance moved (cm) was tracked (uninfected n=63, C6706 n=51). Average distance was calculated in Excel from 1 second time bins and analyzed on GraphPad using Mann-Whitney test with $p < 0.05$ as cutoff for significance.

2.6. Zebrafish Euthanization and Homogenization

All larvae were euthanized in a lethal dose of MS-222 (300 mg/L Tris buffer, pH 7.0) for 30 minutes and homogenized with a pellet pestle (Fisher Scientific, Pittsburgh, PA). Before infection at 5 dpf, 15 larvae were homogenized together in 100 µL of 1x PBS. At 10 dpf, 5 uninfected larvae and 5 C6706-infected larvae were homogenized together in 100 µL of 1x PBS.

2.7. DNA Isolation and Sequencing

DNA from 100 μL of larval zebrafish's combined homogenate was isolated using the DNEasy Powersoil Pro kit (Qiagen, Germantown, MD) per the manufacturer's instructions. Two extractions using only sterile 1x PBS and no gut samples were also processed as kit controls. The V4 region of the 16s rRNA gene was targeted and amplified using 515F and 806R primers. These primers have yielded successful results in previous zebrafish microbiome studies, and the V4 region has demonstrated high reproducibility [45,51]. Samples were submitted to Michigan State University for Illumina MiSeq Sequencing using previously established methods [52,53].

All raw data were processed with R package 'dada2tools', available at https://github.com/jp589/dada2tools, to efficiently correct Illumina amplicon errors without generating operational taxonomic units. Instead, amplicon sequence variants (ASVs) are derived based on 100% sequence similarity. Modifications to an online MiSeq protocol (https://benjjneb.github.cio/dada2/tutorial.html) included allowing truncation lengths of 245 bp and 210 bp and a maximum number of errors of 2 bp for forward reads and 7 bp for reverse reads. Sequences were then classified into taxa using the silva_nr99_v138.1_train_set database with a minimum bootstrap value of 80% [54]. classified as mitochondrial, chloroplast, or not classified at phylum level were removed. Based on the bacterial profiles of two blank DNA extraction kit samples, 1 ASV, an unclassified *Corynebacterium*, was further removed from the dataset (https://github.com/jp589/dada2tools).

65 ASVs were detected in the larval gut microbiome. The samples of the gut microbiome of larvae at time zero yielded far fewer 16S rRNA gene sequencing reads (6772) than those of either uninfected control (252,894) or C6706 (181,224) larvae at five days post-infection. Thus, relative abundance data were used for descriptive comparisons among these three groups of samples.

3. Results

3.1. Light/Dark Trials

From the light/dark assay between uninfected larvae and C6706-colonized larvae, there was no significant difference in the average distance travelled nor average velocity of either condition (Figure 1A, 1B). Data distribution during the second cycle establishes the non-significant difference (Figure 1C and 1D). This trend continued throughout all four cycles.
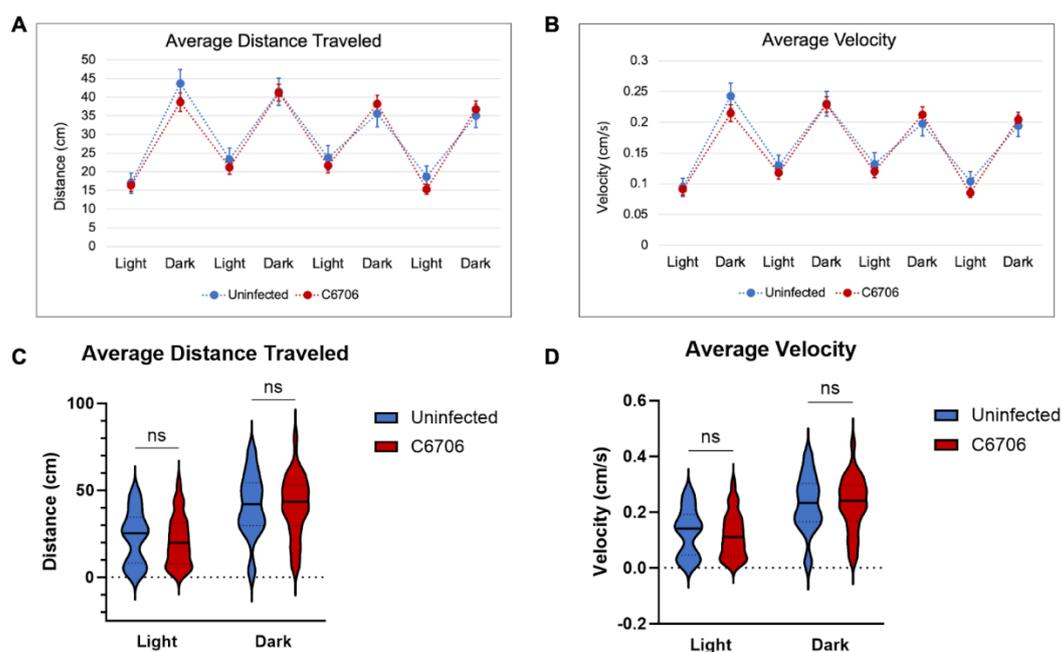

Figure 1. Light/Dark Trial Results. **(A)** Average distance traveled during 4 alternating periods of 3 minutes light and 3 minutes dark. Uninfected control in blue (n=25) and C6706-infected in red (n=60).

(B) Average velocity during 4 alternating periods of 3 minutes light and 3 minutes dark. Uninfected control in blue (n=25) and C6706-infected in red (n=60). Error bars represent standard error of mean. **(C)** Violin plot of average distance traveled during the second cycle of light and dark. **(D)** Violin plot of average velocity during second cycle of light and dark. "ns" indicates no significance.

3.2. Single-Tap Trials

From the single-tap assay, C6706-colonized larvae presented a significantly lower average distance traveled during the 1 second immediately after the single-tap, when compared to the uninfected larvae (Figure 2).
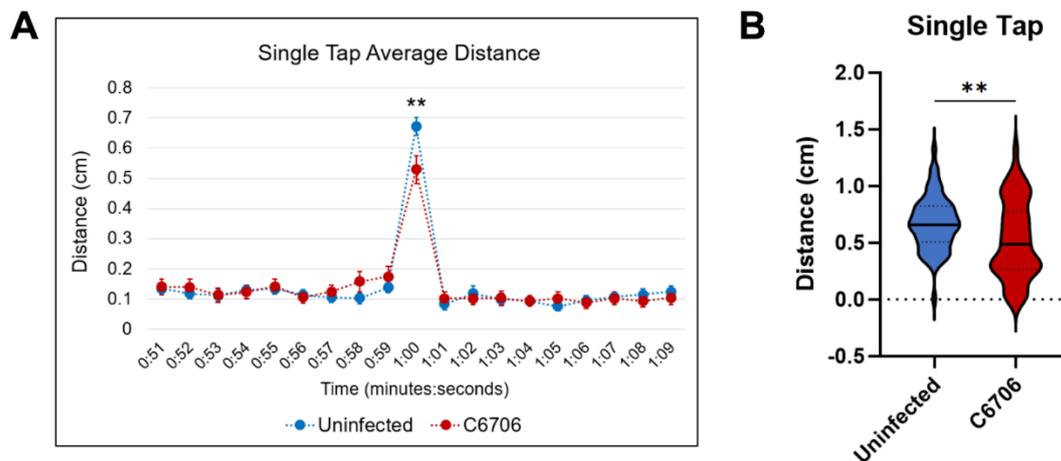

Figure 2. Single-tap trial results. **(A)** Uninfected control in blue (n=63) and C6706-infected in red (n=51). **p=.0092. Student's *t*-test performed for statistical significance. Error bars represent standard error of mean. **(B)** Violin plot of average distance traveled during single tap. "**" indicates p<0.01.

3.3. Larval Gut Microbiome

The two most abundant bacterial ASVs in the guts of larvae at time zero were mainly Proteobacteria, more specifically, an unclassified *Comamonadaceae* (41%) and *Brevundimonas kwangchunensis* (35%). At 5 dpi, the same unclassified *Comamonadaceae* ASV constituted 14% and 7% of the gut microbiomes of uninfected larvae and C6706-infected larvae, respectively. *B. kwangchunensis* constituted less than 1% of both larval groups' microbiomes at this same timepoint. Only one other ASV, an unclassified *Pseudomonas*, constituted more than 5% of the gut microbiome of larvae at time zero. This ASV was the most prominent one among the gut microbiomes of both uninfected (24%) and C6706 (26%) larvae at 5 days post-infection). Notably, these two larval groups shared each of their top 5 ASVs, each constituting at least 5% of their gut microbiome profiles. The taxa of the remaining 4 ASVs were *Rheinheimera coerulea*, unclassified *Flectobacillus*, and two unclassified *Comamonadaceae* (Figure 3).
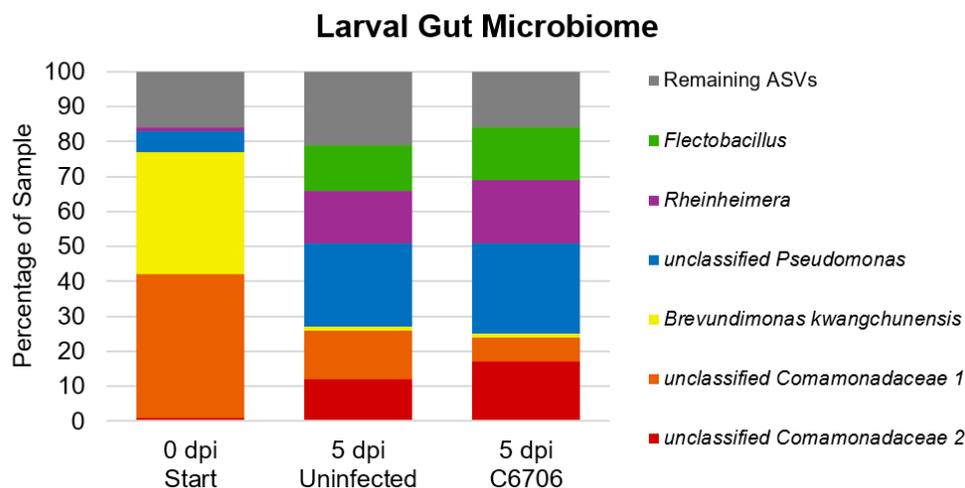
Figure 3. Stacked bar graph of most abundant ASVs identified in larval gut microbiome samples. "Remaining ASVs" refers to all ASVs that constitute less than 5% of the sample.

4. Discussion

The larval zebrafish brain has approximately 100,000 neurons [55]. Identifying a dampened motor response in C6706-colonized larvae to an acoustic stimulus, but not to visual stimuli, could indicate that the gut microbiome has crosstalk with different regions and neurons of the larval brain. An open-source Zbrain atlas of the larval zebrafish brain has been established, opening the door for neuronal activity mapping [55]. Acoustic stimuli were found to activate the ears and lateral line, which directly connects to the octavolateralis nucleus (ON), as well as particularly strong neuron activations in the torus semicircularis, thalamus, cerebellum, and remaining hindbrain [55–58]. Visual stimulus in the form of a 10 second light flash activated the retinal projections and diencephalic areas of the larval brain [55]. In relation to our data, this could indicate a more direct pathway between the gut microbiome and the larval brain regions associated with a response to an acoustic stimulus. More specifically, a *V. cholerae* El Tor C6706-colonized gut microbiome is either indirectly or directly weakening crosstalk due to the presence of C6706 or absence of resident gut microbiota. Larval locomotion studies are translational in that activation of reticulospinal neurons in the brain stem and the vestibulospinal tract are conserved in vertebrates [59]. Structures of the larval zebrafish brain have evolutionarily conserved homologous functions to other vertebrates' [60,61].

Our study aimed to identify any behavioral response from two separate stimuli. Screening for other larval behaviors may yield results highlighting other regions of the brain affected by a gut microbiome shift. This includes multi-tap assays to measure habituation, circadian rhythm assays, and prey-capture to measure decision-making [59,62–65]. Whole-brain imaging would be another direction towards larval neurology during *V. cholerae* colonization. Behavioral studies are also possible for adult zebrafish colonized with *V. cholerae*. While adult zebrafish exhibit much more complex, continuous behaviors, on a broader scale, translational relevance is equally complex [66]. For example, adult zebrafish social phenotypes were parallel to social interaction cues observed in humans, such as head direction and physical distance [67]. A link with *V. cholerae* colonization to behavior in larval and adult zebrafish could translate to environmental observations, where *V. cholerae* and zebrafish potentially interact.

The Comamonadaceae family, *Rheinheimera coerulea*, and Flectobacillus species have been isolated from freshwater environments [68–70]. *Pseudomonas* has been established as a part of the zebrafish core gut microbiome [47]. Stephens et al. has shown that unclassified Comamonadaceae took up 97.5% of all larval intestines [43]. *Brevundimonas kwangchunensis* is the one ASV that has not been thoroughly described, although the *Brevundimonas* genus has been found in soil and water samples [71,72]. It is interesting that *Vibrio* was not one of the most abundant ASVs from the C6706-infected group, though the few larval homogenates plated from this time did yield X-gal blue CFUs

indicative of *V. cholerae* (not shown). It could be possible that the specific group of larval homogenates submitted for sequencing were poorly infected and colonized with *V. cholerae* in comparison to other larvae. The gut microbiome abundances and number of ASVs significantly changing from 5 dpf to 10 dpf prove that gut microbiome diversity can quickly shift at this early developmental stage [43]. Additionally, perhaps plating homogenates on LB without streptomycin would provide confirmation of other, more abundant bacterial species' growth. Since these behavioral analyses were the first to consider *V. cholerae*, future trials can include more larvae for sampling to provide a more comprehensive model of the gut microbiome.

In terms of *V. cholerae* colonization, while V. cholerae El Tor C6706 was tested, it is possible that classical and non-O1 biotype strains induce different behavioral responses. Future studies could determine if interactions between the larval gut and brain play a role specific to the more persistent colonization of *V. cholerae* El Tor strains.

Author Contributions: I.C., R.T. and J.H.W.; methodology, X.L. and S.B.; software, X.L. and S.B.; validation, I.C.; formal analysis, I.C.; investigation, I.C.; resources, X.L. and R.T.; data curation, I.C., K.R.T. and J.P..; writing—original draft preparation, I.C.; writing—review and editing, I.C., J.P. and J.H.W.; visualization, I.C.; supervision, J.H.W.; project administration, R.T. and J.H.W.; funding acquisition, J.H.W. All authors have read and agreed to the published version of the manuscript.

Conflicts of Interest: The authors declare no conflicts of interest.

References

1. Kaper, J.B., J.G. Morris, Jr., and M.M. Levine, *Cholera.* Clin Microbiol Rev, 1995. **8**(1): p. 48-86.
2. Sack, D.A., et al., *Cholera.* The Lancet, 2004. **363**(9404): p. 223-233.
3. WHO. *Number of reported cholera cases.* 2017 September 18, 2017 [cited 2020 December 1]; Available from: https://www.who.int/gho/epidemic_diseases/cholera/cases_text/en/.
4. Organization, W.H., *Cholera Annual Report 2020 Weekly Epidemiological Record 37.* 2021. **96**: p. 445-460.
5. Organization, W.H., *Cholera – Global situation.* 2023. **Disease Outbreak News**.
6. Vezzulli, L., et al., *Climate influence on Vibrio and associated human diseases during the past half-century in the coastal North Atlantic.* Proc Natl Acad Sci U S A, 2016. **113**(34): p. E5062-71.
7. Sack, D.A., et al., *Cholera.* Lancet, 2004. **363**(9404): p. 223-33.
8. Kirn, T.J. and R.K. Taylor, *TcpF is a soluble colonization factor and protective antigen secreted by El Tor and classical O1 and O139 Vibrio cholerae serogroups.* Infect Immun, 2005. **73**(8): p. 4461-70.
9. Faruque, S.M., M.J. Albert, and J.J. Mekalanos, *Epidemiology, genetics, and ecology of toxigenic Vibrio cholerae.* Microbiol Mol Biol Rev, 1998. **62**(4): p. 1301-14.
10. Herrington, D.A., et al., *Toxin, toxin-coregulated pili, and the toxR regulon are essential for Vibrio cholerae pathogenesis in humans.* J Exp Med, 1988. **168**(4): p. 1487-92.
11. Thelin, K.H. and R.K. Taylor, *Toxin-coregulated pilus, but not mannose-sensitive hemagglutinin, is required for colonization by Vibrio cholerae O1 El Tor biotype and O139 strains.* Infect Immun, 1996. **64**(7): p. 2853-6.
12. Torgersen, M.L., et al., *Internalization of cholera toxin by different endocytic mechanisms.* J Cell Sci, 2001. **114**(Pt 20): p. 3737-47.
13. Harris, J.B., et al., *Cholera.* Lancet, 2012. **379**(9835): p. 2466-2476.
14. Smirnova, N.I., et al., *Molecular-genetic peculiarities of classical biotype Vibrio cholerae, the etiological agent of the last outbreak Asiatic cholera in Russia.* Microb Pathog, 2004. **36**(3): p. 131-9.
15. Ghosh, P., et al., *Haitian Variant Vibrio cholerae O1 Strains Manifest Higher Virulence in Animal Models.* Front Microbiol, 2019. **10**: p. 111.
16. Satchell, K.J., et al., *Phenotypic Analysis Reveals that the 2010 Haiti Cholera Epidemic Is Linked to a Hypervirulent Strain.* Infect Immun, 2016. **84**(9): p. 2473-81.
17. Samanta, P., et al., *Dissemination of newly emerged polymyxin B sensitive Vibrio cholerae O1 containing Haitian-like genetic traits in different parts of India.* J Med Microbiol, 2018. **67**(9): p. 1326-1333.

18. Qin, J., et al., *A human gut microbial gene catalogue established by metagenomic sequencing.* Nature, 2010. **464**(7285): p. 59-65.

19. Sender, R., S. Fuchs, and R. Milo, *Are We Really Vastly Outnumbered? Revisiting the Ratio of Bacterial to Host Cells in Humans.* Cell, 2016. **164**(3): p. 337-340.

20. Arumugam, M., et al., *Enterotypes of the human gut microbiome.* Nature, 2011. **473**(7346): p. 174-80.

21. Faith, J.J., et al., *Predicting a human gut microbiota's response to diet in gnotobiotic mice.* Science, 2011. **333**(6038): p. 101-4.

22. Schmidt, T.S.B., J. Raes, and P. Bork, *The Human Gut Microbiome: From Association to Modulation.* Cell, 2018. **172**(6): p. 1198-1215.

23. Kashyap, P.C., et al., *Genetically dictated change in host mucus carbohydrate landscape exerts a diet-dependent effect on the gut microbiota.* Proc Natl Acad Sci U S A, 2013. **110**(42): p. 17059-64.

24. Li, H., et al., *The outer mucus layer hosts a distinct intestinal microbial niche.* Nature Communications, 2015. **6**(1): p. 8292.

25. Sicard, J.F., et al., *Interactions of Intestinal Bacteria with Components of the Intestinal Mucus.* Front Cell Infect Microbiol, 2017. **7**: p. 387.

26. Khan, M.U., et al., *Cholera, rotavirus and ETEC diarrhoea: some clinico-epidemiological features.* Transactions of The Royal Society of Tropical Medicine and Hygiene, 1988. **82**(3): p. 485-488.

27. Hsiao, A., et al., *Members of the human gut microbiota involved in recovery from Vibrio cholerae infection.* Nature, 2014. **515**(7527): p. 423-426.

28. David, L.A., et al., *Gut microbial succession follows acute secretory diarrhea in humans.* mBio, 2015. **6**(3): p. e00381-15.

29. Chen, Y., J. Xu, and Y. Chen, *Regulation of Neurotransmitters by the Gut Microbiota and Effects on Cognition in Neurological Disorders.* Nutrients, 2021. **13**(6).

30. Silva, Y.P., A. Bernardi, and R.L. Frozza, *The Role of Short-Chain Fatty Acids From Gut Microbiota in Gut-Brain Communication.* Front Endocrinol (Lausanne), 2020. **11**: p. 25.

31. Breit, S., et al., *Vagus Nerve as Modulator of the Brain-Gut Axis in Psychiatric and Inflammatory Disorders.* Front Psychiatry, 2018. **9**: p. 44.

32. Diaz Heijtz, R., et al., *Normal gut microbiota modulates brain development and behavior.* Proc Natl Acad Sci U S A, 2011. **108**(7): p. 3047-52.

33. Neufeld, K.M., et al., *Reduced anxiety-like behavior and central neurochemical change in germ-free mice.* Neurogastroenterology & Motility, 2011. **23**(3): p. 255-e119.

34. Spira, W.M., R.B. Sack, and J.L. Froehlich, *Simple adult rabbit model for Vibrio cholerae and enterotoxigenic Escherichia coli diarrhea.* Infection and immunity, 1981. **32**(2): p. 739-747.

35. Burrows, W. and G.M. Musteikis, *Cholera infection and toxin in the rabbit ileal loop.* J Infect Dis, 1966. **116**(2): p. 183-90.

36. Withey, J.H., et al., *Conjugated Linoleic Acid Reduces Cholera Toxin Production* In Vitro *and* In Vivo *by Inhibiting Vibrio cholerae ToxT Activity.* Antimicrob Agents Chemother, 2015. **59**(12): p. 7471-6.

37. Matson, J.S., *Infant Mouse Model of Vibrio cholerae Infection and Colonization*, in *Vibrio Cholerae: Methods and Protocols*, A.E. Sikora, Editor. 2018, Springer New York: New York, NY. p. 147-152.

38. Nygren, E., et al., *Establishment of an adult mouse model for direct evaluation of the efficacy of vaccines against Vibrio cholerae.* Infect Immun, 2009. **77**(8): p. 3475-84.

39. Sawasvirojwong, S., et al., *An Adult Mouse Model of Vibrio cholerae-induced Diarrhea for Studying Pathogenesis and Potential Therapy of Cholera.* PLoS Negl Trop Dis, 2013. **7**(6): p. e2293.

40. Runft, D.L., et al., *Zebrafish as a natural host model for Vibrio cholerae colonization and transmission.* Applied and environmental microbiology, 2014. **80**(5): p. 1710-1717.

41. Mitchell, K.C. and J.H. Withey, *Danio rerio as a Native Host Model for Understanding Pathophysiology of Vibrio cholerae*, in *Vibrio Cholerae: Methods and Protocols*, A.E. Sikora, Editor. 2018, Humana Press Inc: Totowa. p. 97-102.

42. Nag, D., et al., *Quantifying Vibrio cholerae Colonization and Diarrhea in the Adult Zebrafish Model.* J Vis Exp, 2018(137).

43. Stephens, W.Z., et al., *The composition of the zebrafish intestinal microbial community varies across development.* The ISME Journal, 2016. **10**(3): p. 644-654.

44. Senderovich, Y., I. Izhaki, and M. Halpern, *Fish as reservoirs and vectors of Vibrio cholerae.* PLoS One, 2010. **5**(1): p. e8607.

45. Breen, P., et al., *Vibrio cholerae Infection Induces Strain Specific Modulation of the Zebrafish Intestinal Microbiome.* Infect Immun, 2021: p. Iai0015721.

46. Kuil, L.E., et al., *Zebrafish: A Model Organism for Studying Enteric Nervous System Development and Disease.* Frontiers in Cell and Developmental Biology, 2021. **8**.

47. Roeselers, G., et al., *Evidence for a core gut microbiota in the zebrafish.* The ISME Journal, 2011. **5**(10): p. 1595-1608.

48. Davis, D.J., et al., *Microbial modulation of behavior and stress responses in zebrafish larvae*. Behav Brain Res, 2016. **311**: p. 219-227.

49. Phelps, D., et al., *Microbial colonization is required for normal neurobehavioral development in zebrafish*. Scientific Reports, 2017. **7**(1): p. 11244.

50. Banerjee, S., et al., *Vision and sensorimotor defects associated with loss of Vps11 function in a zebrafish model of genetic leukoencephalopathy*. Sci Rep, 2022. **12**(1): p. 3511.

51. Breen, P., et al., *Internal Versus External Pressures: Effect of Housing Systems on the Zebrafish Microbiome*. Zebrafish, 2019. **16**(4): p. 388-400.

52. Caporaso, J.G., et al., *Ultra-high-throughput microbial community analysis on the Illumina HiSeq and MiSeq platforms*. The ISME Journal, 2012. **6**(8): p. 1621-1624.

53. Whittaker, D.J., et al., *Social Environment Has a Primary Influence on the Microbial and Odor Profiles of a Chemically Signaling Songbird*. Frontiers in Ecology and Evolution, 2016. **4**(90).

54. Quast, C., et al., *The SILVA ribosomal RNA gene database project: improved data processing and web-based tools*. Nucleic Acids Res, 2013. **41**(Database issue): p. D590-6.

55. Randlett, O., et al., *Whole-brain activity mapping onto a zebrafish brain atlas*. Nat Methods, 2015. **12**(11): p. 1039-46.

56. Liao, J.C. and M. Haehnel, *Physiology of afferent neurons in larval zebrafish provides a functional framework for lateral line somatotopy*. J Neurophysiol, 2012. **107**(10): p. 2615-23.

57. Vanwalleghem, G., L.A. Heap, and E.K. Scott, *A profile of auditory-responsive neurons in the larval zebrafish brain*. J Comp Neurol, 2017. **525**(14): p. 3031-3043.

58. Poulsen, R.E., et al., *Broad frequency sensitivity and complex neural coding in the larval zebrafish auditory system*. Curr Biol, 2021. **31**(9): p. 1977-1987.e4.

59. Basnet, R.M., et al., *Zebrafish Larvae as a Behavioral Model in Neuropharmacology*. Biomedicines, 2019. **7**(1).

60. Perathoner, S., M.L. Cordero-Maldonado, and A.D. Crawford, *Potential of zebrafish as a model for exploring the role of the amygdala in emotional memory and motivational behavior*. J Neurosci Res, 2016. **94**(6): p. 445-62.

61. Lucini, C., et al., *BDNF, Brain, and Regeneration: Insights from Zebrafish*. Int J Mol Sci, 2018. **19**(10).

62. Beppi, C., D. Straumann, and S.Y. Bögli, *Author Correction: A model-based quantification of startle reflex habituation in larval zebrafish*. Sci Rep, 2021. **11**(1): p. 8166.

63. Rihel, J., et al., *Zebrafish behavioral profiling links drugs to biological targets and rest/wake regulation*. Science, 2010. **327**(5963): p. 348-51.

64. Borla, M.A., et al., *Prey capture by larval zebrafish: evidence for fine axial motor control*. Brain Behav Evol, 2002. **60**(4): p. 207-29.

65. Banerjee, S., et al., *Hypomyelinated vps16 Mutant Zebrafish Exhibit Systemic and Neurodevelopmental Pathologies*. Int J Mol Sci, 2024. **25**(13).

66. Kalueff, A.V., et al., *Towards a comprehensive catalog of zebrafish behavior 1.0 and beyond*. Zebrafish, 2013. **10**(1): p. 70-86.

67. Stewart, A.M., et al., *Zebrafish models for translational neuroscience research: from tank to bedside*. Trends Neurosci, 2014. **37**(5): p. 264-78.

68. Moon, K., et al., *Genomic and ecological study of two distinctive freshwater bacteriophages infecting a Comamonadaceae bacterium*. Scientific Reports, 2018. **8**(1): p. 7989.

69. Sheu, S.-Y., et al., *Rheinheimera coerulea sp. nov., isolated from a freshwater creek, and emended description of genus Rheinheimera Brettar* et al. *2002*. International Journal of Systematic and Evolutionary Microbiology, 2018. **68**(7): p. 2340-2347.

70. Chen, W.-M., et al., *Flectobacillus fontis sp. nov., isolated from a freshwater spring*. International Journal of Systematic and Evolutionary Microbiology, 2017. **67**(2): p. 336-342.

71. Yoon, J.H., et al., *Brevundimonas kwangchunensis sp. nov., isolated from an alkaline soil in Korea*. Int J Syst Evol Microbiol, 2006. **56**(Pt 3): p. 613-617.

72. Ryan, M.P. and J.T. Pembroke, *Brevundimonas spp: Emerging global opportunistic pathogens*. Virulence, 2018. **9**(1): p. 480-493.